

# Reactive Sputtering Process for CuIn<sub>1-x</sub>Ga<sub>x</sub>Se<sub>2</sub> Thin Film Solar Cells

---

Nae-Man Park, Ho Sub Lee, and Jeha Kim

*CuIn<sub>1-x</sub>Ga<sub>x</sub>Se<sub>2</sub> (CIGS) thin films are grown on Mo/soda lime glass using a reactive sputtering process in which a Se cracker is used to deliver reactive Se molecules. The Cu and (In<sub>0.7</sub>Ga<sub>0.3</sub>)<sub>2</sub>Se<sub>3</sub> targets are simultaneously sputtered under the delivery of reactive Se. The effects of Se flux on film composition are investigated. The Cu/(In+Ga) composition ratio increases as the Se flux increases at a plasma power of less than 30 W for the Cu target. The (112) crystal orientation becomes dominant, and crystal grain size is larger with Se flux. The power conversion efficiency of a solar cell fabricated using an 800-nm CIGS film is 8.5%.*

**Keywords:** Cu(In,Ga)Se<sub>2</sub> (CIGS), solar cell, chalcopyrite, submicron thin film, reactive sputtering.

## I. Introduction

As our dependence on fossil fuels has increased, environmental and economic problems have also increased. Therefore, there is a great deal of interest in renewable energy sources that can help create sustainable economic development. However, no renewable energy source can currently satisfy the planet's vast energy consumption at low cost. Although solar energy is less cost effective than other power generation technologies, such as thermal, water, and nuclear, it has drawn significant attention as a clean and unlimited energy source. To reduce the cost of power generation using solar radiation,

intensive studies have focused on thin-film photovoltaic (PV) devices [1], [2], of which CuIn<sub>1-x</sub>Ga<sub>x</sub>Se<sub>2</sub> (CIGS) PV devices are the most promising, as they have the highest power conversion efficiency and good stability. Many researchers have studied CIGS PV devices using various methods, such as coevaporation, sputtering, electrodeposition, ink printing, and spray pyrolysis [3]-[5]. The coevaporation process generally shows a higher power conversion efficiency than that of other processes [6], but it has a technical challenge in terms of commercialization because it is difficult to make a high-temperature linear source that is able to uniformly evaporate the metal elements Cu, In, and Ga over a wide area. Therefore, research engineers have shown an interest in the sputtering process, which is a well-established method used in wide areas.

In general, a two-step sputtering process is used in the fabrication of CIGS thin films, the first step of which is the deposition of metal elements, and the second step is the post thermal annealing to obtain a CIGS crystal compound from stacked Cu-In-Ga metal layers at an atmosphere of Ar-diluted H<sub>2</sub>Se gas [7]. This two-step process is not cost-effective and lacks high throughput because the reaction time of the second step far exceeds 60 minutes. As a result, a batch process is preferred, which is less attractive compared to an in-line process in mass production. Therefore, we propose a new method to fabricate a CIGS thin film using a one-step reactive sputtering method that is adaptable to an in-line process. The reactive sputtering equipment used is composed of two radio frequency magnetron sputtering guns and a Se cracker. Reactive sputtering normally requires the use of a reactive gas such as H<sub>2</sub>Se. However, H<sub>2</sub>Se gas is toxic, and an extra treatment system is needed before disposal. Therefore, instead of H<sub>2</sub>Se gas, we use a Se cracker to improve the reactivity of metallic Se. The Se cracker thermally breaks up bulky

Manuscript received Feb. 9, 2012; revised June 26, 2012; accepted July 9, 2012.

This work was supported by the New & Renewable Energy of the Korea Institute of Energy Technology Evaluation and Planning (KETEP) grant funded by the Korea government Ministry of Knowledge Economy (No. 20093020010030). N.-M. Park would like to thank H.G Father for his guidance.

Nae-Man Park (phone: +82 42 860 5987, nmpark@etri.re.kr) and Ho Sub Lee (lhs4leaf@naver.com) are with the Convergence Components & Materials Research Laboratory, ETRI, Daejeon, Rep. of Korea.

Jeha Kim (jeha@cju.ac.kr) was with the Convergence Components & Materials Research Laboratory, ETRI, Daejeon, Rep. of Korea, and is now with the Research Institute of Photovoltaics, Cheongju University, Cheongju, Rep. of Korea.  
<http://dx.doi.org/10.4218/etrij.12.0212.0062>

evaporated Se molecules from the reservoir. To deliver Ar gas onto the target surface to reduce as much of the contamination caused by cracked Se molecules as possible, we use a magnetron sputtering gun that we designed. Using this reactive sputtering system, we study the CIGS film growth and fabricate a solar cell using a submicron-thick CIGS film. Development of a submicron-thick CIGS absorber showing a high efficiency is also an interesting topic because this development can reduce manufacturing cost. The coevaporation process shows power conversion efficiency of about 10% to 12% in a 600-nm CIGS film with antireflection coating [8], [9]. Our solar cell shows power conversion efficiency of over 8% in an 800-nm CIGS film without antireflection coating.

## II. Experiment

Cu and  $(In_{0.7}Ga_{0.3})_2Se_3$  targets and a Se cracker are used to fabricate CIGS thin film on Mo/soda lime glass (SLG). The process temperature and pressure are 500°C and 8 mTorr, respectively. A Mo film of 900 nm is deposited onto the SLG (25 mm × 25 mm × 1.1 mm polished glass) at a pressure of 2 mTorr at room temperature using a DC magnetron sputtering process at 300 W. The  $(In_{0.7}Ga_{0.3})_2Se_3$  target is simultaneously sputtered with a Cu target by radio frequency magnetron guns at a fixed power of 100 W. The Cu target is sputtered with a power variation of 25 W to 40 W for the CIGS compound film. The Se cracker (model: SCS-500D) is composed of a Se evaporation reservoir and a cracking zone for pyrolyzing evaporated bulky Se molecules. The reservoir temperature is adjusted from 210°C to 310°C to control the Se flux, and the cracking zone is maintained at 900°C.

CIGS thin films are characterized by X-ray fluorescence spectroscopy (XRF) using a Solar Metrology SMX-BEN to obtain their information of composition and thickness. X-ray diffraction (XRD) is performed using a Rigaku D/Max-RC Bede/DCC300 with Cu K $\alpha$  ( $\lambda=1.54$  Å) radiation. XRD data is collected at 0.02 increments of  $2\theta$  at a scan rate of 3° per minute with a  $\theta$ -2 $\theta$  goniometer and a sample rotation of 60 revolutions per minute. Scanning electron microscopy (SEM) images are obtained using an FEI Sirion 400 operating at 10 KeV to confirm the film thickness and the crystal grain size. No metallic coating is carried out.

For PV device fabrication, a CdS buffer layer is deposited onto the CIGS/Mo/SLG at 50°C in a bath containing 300 ml of DI water, 0.015 M of CdSO<sub>4</sub>, 0.75 M of thiourea, and 56 ml of NH<sub>3</sub> (28%). The reaction is carried out for eight minutes. After completion of the procedure, the samples are washed by DI water and blow-dried using nitrogen gas. An ITO/i-ZnO window layer is deposited by radio frequency magnetron

sputtering using ZnO (99.9%) and ITO (99.99%, In<sub>2</sub>O<sub>3</sub>:SnO<sub>2</sub> = 90:10) targets. A 70-nm-thick i-ZnO film is deposited in an Ar atmosphere with 25% O<sub>2</sub> at a pressure of 30 mTorr using a power of 400 W at ambient temperature. A 150-nm-thick ITO film is deposited in an Ar atmosphere of 50 mTorr with a power of 100 W at 200°C. An Al/Ni (3,000/50 nm) top grid contact is deposited by using an e-beam evaporator. The final active region of the device is 0.47 cm<sup>2</sup> (1 cm × 0.5 cm). The power conversion efficiency is measured using a solar simulator (Oriel 91193-1000) equipped with an AM 1.5 filter.

## III. Results and Discussion

Figure 1(a) shows the Se flux variation as a function of the reservoir temperature of the Se cracker when the cracking zone temperature is fixed at 900°C. The monitoring position of the Se flux is 300 mm away from the end of the cracking zone, whereas the film deposition occurs within 260 mm of the end of the cracking zone. During the film deposition, the Se is uniformly deposited over an area of 300 mm × 300 mm. Therefore, the Se flux in Fig. 1(a) is a relative value. The relative Se flux varies from 0.13 Å/s to 11 Å/s as the reservoir temperature increases from 230°C to 310°C. The Se flux is linearly proportional to the reservoir temperature at the log scale, and we are able to easily control the Se flux by varying this reservoir temperature. This Se cracker is a downward type, and the Se vapor of the reservoir zone is maintained at a high pressure compared to that of an upward type, which is able to supply a uniform Se vapor over a long period. In our case, a uniform rate is sustained for eight hours.

Figure 1(b) shows the ratio of Cu to In+Ga contents (Cu/III) in a CIGS film with variations in the reservoir temperature of the Se cracker. The reservoir temperature of the Se cracker corresponds to the Se flux, as shown in Fig. 1(a). Using this

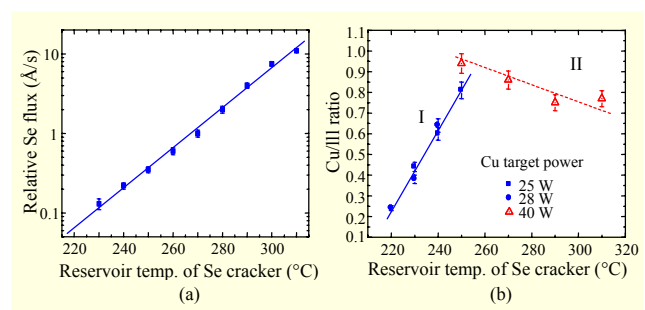
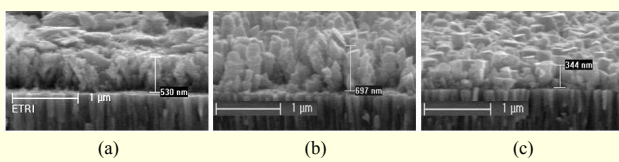
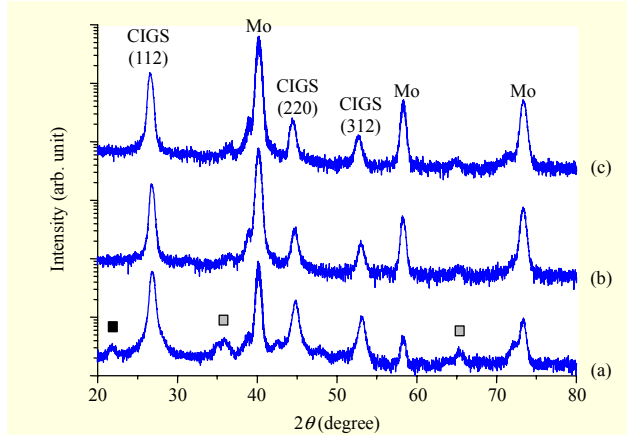


Fig. 1. (a) Relative Se flux as function of reservoir temperature of Se cracker at cracking temperature of 900°C. Se flux is linearly proportional to reservoir temperature at log scale. (b) Cu/III ratio as function of reservoir temperature of Se cracker. Reservoir temperature corresponds to Se flux. Cu/III ratio increases in region I and decreases in region II with increase in Se flux.



**Fig. 2.** SEM images of CIGS films with different Cu contents in region I: (a) Cu/III = 0.24, (b) Cu/III = 0.64, and (c) Cu/III = 0.81. Crystal grain becomes larger as Cu/III ratio increases. Scale bar is same in all images.



**Fig. 3.** XRD patterns of same sample series shown in Fig. 2: (a) Cu/III = 0.24, (b) Cu/III = 0.64, and (c) Cu/III = 0.81. Three peaks related to CIGS crystal are shown. Two peaks (gray squares) shown at 35.8° and 65.3° are related to  $\text{Cu}_{16}\text{In}_9$  (JCPDS 26-0522), and peak (black square) shown at 21.8° is related to  $\eta\text{-}(\text{Cu}_2\text{Se})_{0.09}(\text{In}_2\text{Se}_3)_{9.91}$  (JCPDS 39-7059).

one-step process, a CIGS compound film is produced through the cosputtering of Cu and  $(\text{In}_{0.7}\text{Ga}_{0.3})_2\text{Se}_3$  targets with the assistance of the Se supply. An Ar atmosphere is consistently maintained at 8 mTorr during the sputtering of two targets, and Se is supplied via the Se cracker.

The Cu/III ratio decreases as the Se flux increases under a 40-W sputtering power of the Cu target, which is a similar phenomenon observed in the coevaporation process [10], [11]. We keep the reservoir temperature below 310°C to maintain the stability of the Se flux. In region II, Cu metal segregation occurs, and a volatile compound such as  $\text{In}_2\text{Se}$  forms as the Se supply becomes insufficient, which results in an increase in the Cu content of the film [9]. However, the Cu/III ratio increases as the Se flux increases in region I, where the sputtering power of the Cu target is less than 30 W. This behavior has not been observed in the coevaporation process, and there have been few reports on such behavior because the Se source is made up of bulky molecules in the coevaporation process. A bulky molecule has a low reactivity, and it is very difficult to observe a reactive characteristic at a low flux.

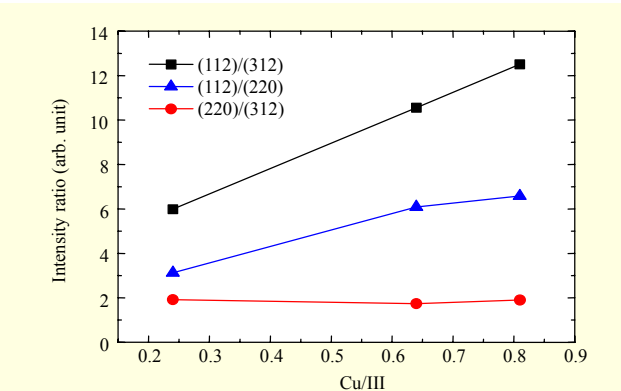


**Fig. 4.** XRD peak intensity ratio of CIGS crystal film to each crystal plane as function of Cu/III shown in Fig. 3. (112) crystal plane becomes dominant with increasing Cu/III compared to other crystal planes.

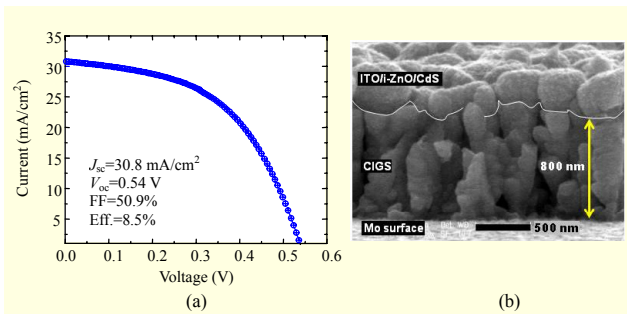


**Fig. 5.** (a) Current-voltage (J-V) curve of solar cell fabricated with 800-nm CIGS film and (b) SEM image of 800-nm CIGS film grown through reactive sputtering. Cu/III and Ga/III ratios are about 0.82 and 0.30, respectively.

Figure 2 shows SEM images of the CIGS films shown in Fig. 1(b) with different Cu contents in region I. All CIGS films are grown on Mo/SLG. As the Cu/III ratio increases from 0.24 to 0.81, the average size of the crystal grains in the CIGS film clearly increases from 100 nm to 200 nm. Therefore, it is likely that a high Cu content facilitates CIGS crystal grain growth. We measure XRD to know which crystal orientation is developing with an increase in the Cu/III ratio (or Se flux).

Figure 3 shows XRD patterns of the same sample series as shown in Fig. 2, where Mo peaks are positioned at 40.1°, 58.3°, and 73.3°, which are related to (110), (200), and (211) crystal orientations in a cubic structure, respectively (JCPDS 42-1120).  $\eta\text{-}(\text{Cu}_2\text{Se})_{0.09}(\text{In}_2\text{Se}_3)_{9.91}$  is observed at 21.8°, and  $\text{Cu}_{16}\text{In}_9$ -related peaks are observed at 35.8° and 65.3° only in sample (a) of Cu/III=0.24. However, the Cu and Se come to sufficiently react with  $(\text{In}_{0.7}\text{Ga}_{0.3})_2\text{Se}_3$  as the Se flux increases, resulting in CIGS crystal grain growth. The indication is that an insufficient Se supply does not form a stable Cu-Se or CIGS compound, and, as a result, a volatile Cu-In(Ga) metallic compound or Cu-

rich selenide such as  $\text{Cu}_{2-x}\text{Se}$  or  $\text{CuSe}$  develops during the CIGS film deposition [12], [13], which causes a decrease in the Cu content of the film. The three CIGS peaks in sample (a) can be considered as a  $\text{Cu}(\text{In},\text{Ga})_3\text{Se}_5$  crystal due to the low Cu content. The  $\text{Cu}(\text{In},\text{Ga})_3\text{Se}_5$  phase has a very similar lattice parameter but characteristic peaks due to (002), (110), (200), (202), and (114) planes [14]. Considering that XRF provides information of an overall film composition and there is no characteristic peak related to the  $\text{Cu}(\text{In},\text{Ga})_3\text{Se}_5$  phase in Fig. 3(a), it is reasonable that we assign CIGS phases to these peaks.

CIGS crystallinity is also changed according to variation in the Se flux. Figure 4 shows the XRD peak intensity ratio of CIGS crystals for each crystal orientation as a function of Cu/III. When CIGS crystallinity becomes dominant in the (112) orientation as Cu/III increases, there is no dependency of the (220) and (312) orientations on the Se flux. Considering thermodynamics, the (112) orientation is preferred. Crystal grain growth makes it possible to develop a crystal grain film with a (112) orientation under sufficient Se conditions [15].

Figure 5 shows the power conversion efficiency of a solar cell fabricated with an 800-nm CIGS film at a Cu/III ratio of 0.82 and a Ga/III ratio of 0.30. In the coevaporation process, the optimum condition to show a high efficiency is Cu/III of 0.9 and Ga/III of 0.3 in a CIGS film composition [15], but the best efficiency is acquired in a different film composition in a reactive sputtering process. The short-circuit current density is 30.8 mA/cm<sup>2</sup>, but the open-circuit voltage of 0.54 V is somewhat low considering Ga/III. The fill factor is also low. In the SEM image, the density of the CIGS crystal grain appears to be low and the crystal grain size is small compared to that of the sample grown through the coevaporation process [16], which is attributed to the low fill factor. Therefore, we need to further optimize the process condition to obtain a dense and large crystal grain film. However, the power conversion efficiency of 8.5% for this 800-nm-thick CIGS solar cell is the highest efficiency ever reported in a submicron-thick CIGS solar cell when using a sputtering process.

#### IV. Conclusion

In this letter, we investigated the effects of a Se flux on a CIGS film composition, particularly the Cu/III ratio in a reactive sputtering system in which a Se cracker was used to supply the reactive Se molecules. As the Se flux increased, the Cu/III ratio also increased, and the (112) crystal orientation became dominant at a sputtering power below 30 W for the Cu target. The crystal grain size was also larger with the Se flux. An 800-nm-thick CIGS solar cell showed a power conversion efficiency of 8.5%.

#### References

- [1] M. Green, "Thin-Film Solar Cells: Review of Materials, Technologies and Commercial Status", *J. Mater. Sci.*, vol. 18, 2007, pp. 15-19.
- [2] F. Krebs, "Fabrication and Processing of Polymer Solar Cells: A Review of Printing and Coating Techniques," *Sol. Energy Mater. Sol. Cells*, vol. 93, 2009, pp. 394-412.
- [3] M. Kemell, M. Ritala, and M. Leskela, "Thin Film Deposition Methods for  $\text{CuInSe}_2$  Solar Cells," *Crit. Rev. Solid State Mat. Sci.*, vol. 30, 2005, pp. 1-31.
- [4] T. Todorov and D. Mitzi, "Direct Liquid Coating of Chalcopyrite Light-Absorbing Layers for Photovoltaic Devices," *Eur. J. Inorg. Chem.*, 2010, pp. 17-28.
- [5] N.-M. Park et al., "Effect of Se flux on  $\text{CuIn}_{1-x}\text{Ga}_x\text{Se}_2$  Film in Reactive Sputtering Process," *Prog. Photovolt: Res. Appl.*, DOI: 10.1002/pip.1202.
- [6] S. Niki et al., "CIGS Absorbers and Processes," *Prog. Photovolt: Res. Appl.*, vol. 18, 2010, pp. 453-466.
- [7] N. Dhere, "GW/Year of CIGS Production within the Next Decade," *Sol. Energy Mater. Sol. Cells*, vol. 91, 2007, pp. 1376-1382.
- [8] K. Ramanathan et al., "Processing and Properties of Sub-micron CIGS Solar Cells," *Proc. 4th World Conf. Photovoltaic Solar Energy Conversion*, 2006, pp. 380-383.
- [9] Z. Jehl et al., "Thinning of CIGS Solar Cells: Part II: Cell Characterizations," *Thin Solid Films*, vol. 519, 2011, pp. 7212-7215.
- [10] S. Chaisitsak, A. Yamada, and M. Konagai, "Preferred Orientation Control of  $\text{Cu}(\text{In}_{1-x}\text{Ga}_x)\text{Se}_2$  ( $x \approx 0.28$ ) Thin Films and Its Influence on Solar Cell Characteristics," *Jpn. J. Appl. Phys.*, vol. 41, 2002, pp. 507-513.
- [11] G. Hanna et al., "Influence of the Selenium Flux on the Growth of  $\text{Cu}(\text{In},\text{Ga})\text{Se}_2$  Thin Films," *Thin Solid Films*, vol. 431-432, 2003, pp. 31-36.
- [12] A. Bolcavage et al., "Phase Equilibria of the cu-in System I: Experimental Investigation," *J. Phase Equilibria*, vol. 14, 1993, pp. 14-21.
- [13] R. Murray and R. Heyding, "The Copper-Selenium System at Temperatures to 850 K and Pressures to 50 kbar," *Can. J. Chem.*, vol. 53, 1975, pp. 878-887.
- [14] W. Honle, G. Huhn, and U. Boehnke, "Crystal Structures of Two Quenched  $\text{CuInSe}$  Phases," *Cryst. Res. Technol.*, vol. 23, 1988, pp. 1347-1354.
- [15] T. Schlenker et al., "Substrate Influence on  $\text{Cu}(\text{In},\text{Ga})\text{Se}_2$  Film Texture," *Thin Solid Films*, vol. 480-481, 2005, pp. 29-32.
- [16] Y.-D. Chung et al., "Incorporation of Cu in  $\text{Cu}(\text{In},\text{Ga})\text{Se}_2$ -Based Thin-Film Solar Cells," *J. Kor. Phys. Soc.*, vol. 57, 2010, pp. 1826-1830.